17th Australasian Fluid Mechanics Conference
Auckland, New Zealand
5-9 December 2010

Skin Friction Measurement in Zero and Adverse Pressure Gradient Boundary Layers Using Oil Film Interferometry

R. Madad, Z. Harun, K. Chauhan, J.P. Monty and I. Marusic

Department of Mechanical Engineering
The University of Melbourne, Parkville, Victoria, 3010 Australia

Abstract

Skin friction and velocity measurements were measured in zero and adverse pressure gradient boundary layers using oil-film interferometry and single hot-wire sensors. Oil-film interferograms were analyzed using the Empirical Mode Decomposition (EMD) and Hilbert transform techniques [9] that, in contrast to commonly used Fourier based techniques, are less subjective and superior for treating amplitude and frequency modulated data [4]. As an independent technique, the oil-film measurement has been used to assess the use of the Clauser-chart [5]. For strong pressure gradients, at the Reynolds numbers considered here, the Clauser-chart results were found to underestimate the wall-shear stress velocity as found by oil-film interferometry.

Introduction

The contribution of skin friction is a significant part of the total drag in almost all transportation systems. The measurement of skin friction is therefore important for applied problems, such as improving the performance of transportation vehicles and fundamental problems, such as characterizing surface flows.

The assessment of the wall-shear stress, $\tau = \mu \cdot \partial U/\partial z$, has been the subject of many experimental and numerical studies. Here μ is the dynamic fluid viscosity, U the streamwise velocity, and z the distance from the wall. The knowledge of the mean wall-shear stress is a necessary prerequisite to determine the friction velocity, $u_\tau = (\tau/\rho)^{1/2}$, as one of the fundamental turbulence scaling parameters. The temporal and spatial shear stress distribution is related to turbulent flow structures in the vicinity of the wall and is as such of major importance for the basic understanding of the development of near-wall turbulent events.

It is not certain that the standard logarithmic law of the wall holds in adverse pressure gradient (APG) flows. In fact, such a pressure-gradient-dependence of the logarithmic region has been observed and reported in the literature, notably by Bourassa and Thomas [2], Spalart and Leonard [16], Nickels [12], Dixit and Ramesh [6], Chauhan *et al.* [3] and Nagib and Chauhan [11].

Skin friction estimation by the Clauser chart method relies on the universal logarithmic law and hence is not suitable for situations where this universality is known to fail. The same holds true for the Preston-tube method even though the details are different.

In the case of strong pressure gradients a shift appears in the profile above or below the conventional log-law associated with a change in the profile's shape, mentioned by Nagano *et al*.[10], Spalart *et al*. [17] and Fernholz *et al*. [8]. In contrast, Skåre and Krogstad [18] and Bernard *et al*. [1] observed that the law of the wall is valid for higher Reynolds number APG flows and for the decelerating flow around an airfoil, respectively.

Oil film interferometry is one of the few methods available for the direct and absolute measurement of skin friction. The technique consists of measuring the thinning rate of an oil film as it is being acted upon by the shear near the wall. This method allows very accurate measurements of the mean skin friction and does not require specific and expensive equipment. A simple camera and monochromatic light source are the only devices needed to perform oil-film interferometry measurements. The utilization of this technique in two-dimensional flows is demonstrated in a number of studies [7, 8, 15, 13, 19].

The aim of this paper is to assess the use of the Clauser-chart for strong pressure gradient flows by using oil-film interferometry as an independent technique.

Experimental Set-Up

Facility

The experiments were performed in an open-return blower wind tunnel with an inlet section area of 940mm $\times$ 375mm. The test section is 4.2m long with an adjustable ceiling. The schematic of the wind tunnel is illustrated in figure 1.

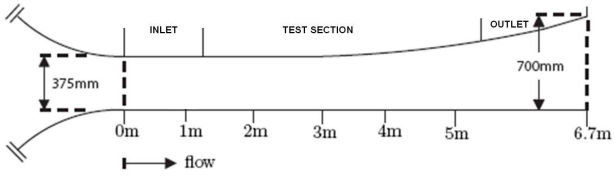

Figure 1: Wind tunnel geometry.

Optical access ports were installed at five stations in the wind tunnel. The first was located in the zero pressure gradient (ZPG) section and the rest in the APG section.

A *Dow Corning* 200 silicon oil droplet with 30 cSt viscosity deposited on the glass plug's surface was illuminated by a sodium lamp mounted underneath. The interference pattern was captured by a digital CCD camera with a 105mm AF Micro *NIKKOR* lens. The viscosity of the oil as a function of temperature was modeled by

$$\nu_{oil} = Ae^{-BT} \tag{1}$$

where, $A = 0.048$ and $B = 0.019$ are the calibration coefficients provided by Rüedi *etal*. [14].

The camera and sodium lamp were mounted on a tripod located under the wind tunnel. It was possible to capture oil-film interferograms from a close distance, resulting in high resolution images.

Image Processing

Numerous techniques exist for the extraction of the fringe spacing from oil-film interferograms. The method used in this study is the Empirical Mode Decomposition (EMD) [9] coupled with

the Hilbert transform which allows one to overcome limitations of Fourier spectral methods to analyze non-stationary and non-linear data series.

The images are captured at a specific time interval and the fringe spacing is the ensemble mean obtained from frequencies estimated from each streamwise pixel line. Since the fringe spacing varies linearly with time, a least square fit gives the slope, dF_s/dt, in pixels. A calibration image is used to convert the pixel space into physical space. Full details of this approach are given by Chauhan *et al* [4].

Pressure Gradient

The pressure gradient in the test section is divided into ZPG and APG sections by adjusting the roof. The pressure coefficient for this setup plotted against the streamwise position in figure 2 shows station 1 under ZPG and the rest under APG.

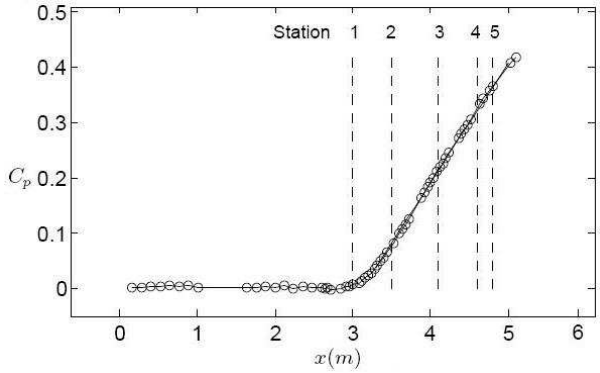

Figure 2: Pressure Coefficient and position of stations.

The commonly used Clauser pressure gradient parameter, β, is defined as,

$$\beta = \frac{\delta^*}{\tau_0}\frac{dP}{dx}, \tag{2}$$

where δ^* is displacement thickness, τ_0 is the wall-shear stress, P is the static pressure and x is the streamwise distance from the inlet. A range of values of this parameter ($0 \leq \beta < 4.8$) were examined in this experiment. Since strong pressure gradients are considered as those in which β is greater than 0.005 [12], the measurement of skin-friction in this experiment is considered for the case of turbulent near-wall flow subjected to a strong adverse pressure gradient.

The skin friction is measured with oil-film interferometry (OFI) technique for three flow cases. The first is a boundary layer evolving under a constant acceleration parameter, $K = (\nu/U_\infty^2)dU_\infty/dx$. The second flow case is an APG flow with constant Reynolds number, $Re_\tau = \delta u_\tau/\nu$, and the third is for the flow with a constant pressure gradient parameter, $\beta \simeq 4.4$.

All these results are compared to skin friction measurements inferred by the Clauser-chart method [5] where, $\kappa = 0.41$ and $A = 5.0$.

Results and Discussion

Skin Friction

The wall skin-friction is commonly expressed in a non-dimensional form by the coefficient of skin friction

$$C_f = \frac{2\tau_w}{\rho U_\infty^2} = 2\left[\frac{u_\tau}{U_\infty}\right]^2. \tag{3}$$

The relationship between the oil-film gradient and the shear force, equation (4), first expressed by Tanner and Blows [19], then with some modifications by Fernholz *et al*. [7] is used.

$$\tau_w = \mu_{oil}\frac{\triangle x}{\triangle t}\frac{2\sqrt{n_{oil}^2 - n_{air}^2 sin^2\theta}}{\lambda}, \tag{4}$$

where, μ_{oil} is the viscosity of the oil, τ_w is the wall shear stress, $\triangle x$ is the fringe spacing difference in distance relative to the leading edge of the oil-film, $\triangle t$ is time difference, λ is the wavelength of the light source, n_{oil} and n_{air} are the refractive indices of the oil and air, respectively and θ is the illumination incidence angle. The root-mean-square error (RMSE) of linear fits to x versus t is less than 1. A small RMSE would indicate that the estimated development of x versus t is in close agreement to the physical linear behavior [4].

Case One

Figure 3 shows that by increasing Re_τ along the stations in APG flow the friction coefficient measured with OFI in constant acceleration parameter, K, becomes much greater than those obtained from the Clauser-chart with increasing pressure gradient strength. All experimental parameters are shown in table 1 where $K \simeq 15.2$.

x(m)	Re_τ	$u_{\tau-Clauser}$	$u_{\tau-OFI}$	$u_{\tau-diff}(\%)$	β
3.5	1910	0.433	0.441	1.8	0.96
4.1	2500	0.475	0.487	2.5	1.67
4.6	3280	0.476	0.515	8.2	3.22
4.8	3630	0.486	0.525	8.0	4.75

Table 1: Experimental parameters for stations 2 to 5 ($K \simeq 15.2$).

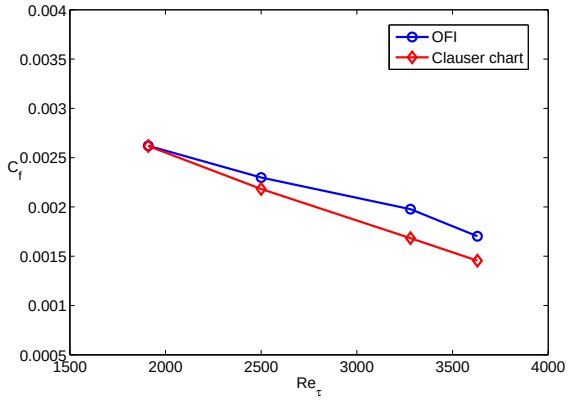

Figure 3: Friction coefficient for matched $K \simeq 15.2$ with increasing Re_τ.

Case Two

Figure 4 demonstrates that the friction coefficient measured by OFI and the Clauser-chart agrees well in ZPG flow (station 1) for matched Reynolds number, Re_τ, where δ is the boundary layer thickness. However, for APG flows the C_f measured with OFI is larger than those obtained from the Clauser-chart. The experimental parameters for the constant Reynolds number are shown in table 2.

Case Three

In order to obtain a flow condition with constant β, the probe remains in station 5 while speed (Re_τ) is increased. The fric-

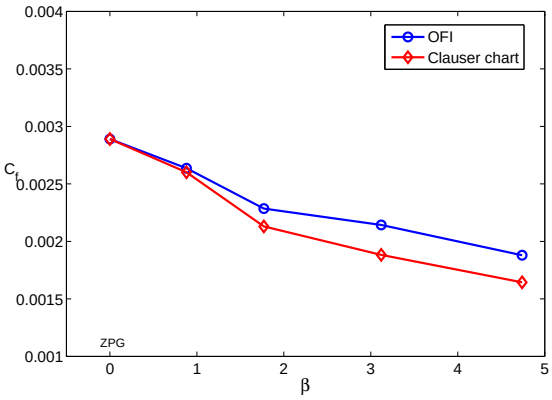

Figure 4: Friction coefficient at a matched $Re_\tau \simeq 1850$.

x(m)	$u_{\tau-Clauser}$	$u_{\tau-OFI}$	β	K
3.0	0.540	0.540	ZPG	ZPG
3.5	0.455	0.458	0.88	-14.1e-8
4.1	0.372	0.385	1.77	-19.4e-8
4.6	0.309	0.327	3.12	-25.6e-8
4.8	0.281	0.305	4.74	-28.2e-8

Table 2: Experimental parameters for stations 1 to 5, for a matched $Re_\tau \simeq 1850$.

tion velocity determined from Clauser-chart, $u_{\tau-Clauser}$, fits to the logarithmic portion of the mean velocity data by using constants κ=0.41 and A = 5.0 compared with the friction velocity measured by OFI, $u_{\tau-OFI}$ (Table 3).

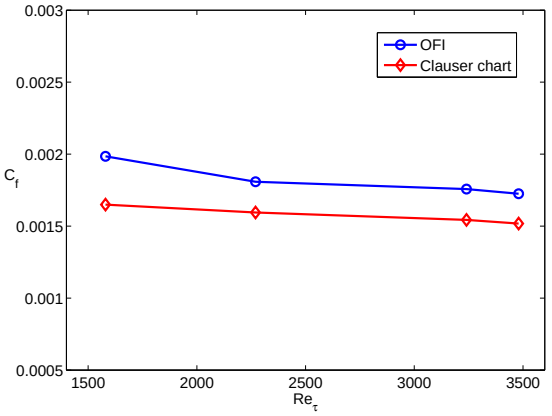

Figure 5: Friction coefficient for matched β ≃ 4.4 with an increasing Re_τ.

Figure 5 illustrates that the coefficient of skin-friction measured with OFI has a shift above the friction coefficient obtained from Clauser-chart for flows at a matched β ≃ 4.4 with increasing Re_τ.

Mean Velocity Profiles

Figure 6 shows the mean velocity profiles normalized by inner scaling for the experiments performed at a matched $Re_\tau \simeq 1850$. The deviation of velocity profiles from conventional log-law could be seen, where by β increasing the logarithmic region is shifted below the standard logarithmic law profile. The overlap parameters, κ and A for these shifted profiles are listed in table 4. We see change in A but κ is almost constant. Nagano

Re_τ	$u_{\tau-Clauser}$	$u_{\tau-OFI}$
1740	0.230	0.258
2500	0.364	0.387
3510	0.475	0.505
3850	0.527	0.573

Table 3: Experimental parameters for station 5 (x=4.8m), where β ≃ 4.4.

et al. [10] showed similar results for the turbulent boundary layer flows where the pressure gradient parameter is maintained at a nearly constant positive value. They also showed that by increasing pressure gradient parameter the constant κ maintained a constant value (κ ≈ 0.4) for the range of $0 < \beta < 4.7$.

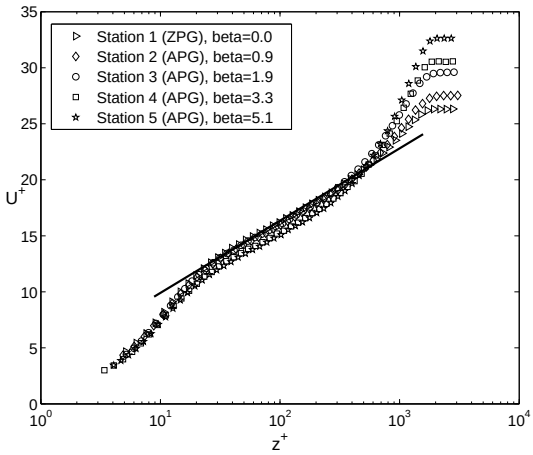

Figure 6: Mean velocity profiles for matched $Re_\tau \simeq 1850$ and varying β.

Station	β	κ	A
1	0	0.399	4.729
2	0.9	0.396	4.318
3	1.8	0.396	4.400
4	3.1	0.405	3.927
5	4.7	0.392	3.341

Table 4: Coefficients κ and A for constant $Re_\tau \simeq 1850$.

Figure 7 shows a collapse in buffer and overlap region for mean velocity profiles for APG flows for a matched β ≃ 4.4. Also, in the wake region it could be seen that the higher Re_τ results in larger wake parameter (higher U^+). The Coefficients κ and A for this set of flow condition are shown in table 5.

While here we show κ to vary, this is due to curve-fitting procedure used, and the underlying assumption that a log-region exists. This may not strictly be the case, and further study with a more refined log-region detection scheme is required for a conclusive result.

Conclusions

The oil-film interferometry method has been used to measure the skin friction along with measurements of mean velocity boundary profiles for zero and strong adverse pressure gradient flows. The friction coefficient obtained from oil-film interferometry and the Clauser-chart for ZPG flows were within ±1%. On the other hand, for APG flows subjected to a strong pressure gradient, the C_f measured by OFI in condition of constant Re_τ, β and K were greater than those obtained with the

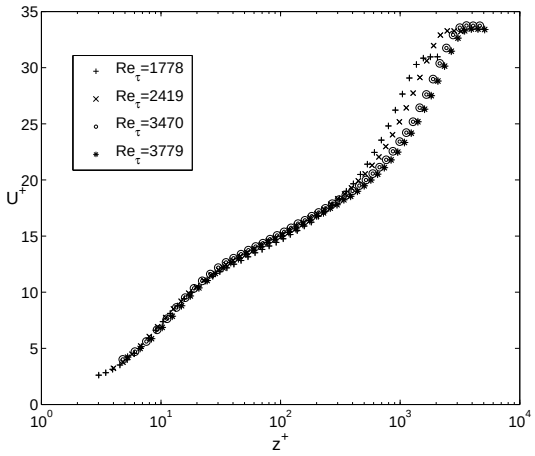

Figure 7: Mean velocity profile for matched $\beta \simeq 4.4$.

Re_τ	κ	A
1778	0.412	3.496
2427	0.401	3.662
3470	0.409	3.969
3779	0.424	4.099

Table 5: Coefficients κ and A for constant $\beta \simeq 4.4$ at station 5.

Clauser-chart. Therefore, it is concluded that Clauser-charts are unreliable for the conditions studied here. That is, for Reynolds numbers ranging from $Re_\tau = 1910$ to $Re_\tau = 3630$ at a matched $K \simeq 15.2$ and for the Reynolds numbers between $Re_\tau = 1740$ and $Re_\tau = 3850$ with constant value of $\beta \simeq 4.4$ there was a little agreement between the results of present experiment and those predicted from the Clauser-chart. The results showed deviation in the mean velocity profile relative to log-law profile for matched Re_τ. Also, by increasing the pressure gradient parameter the constant κ maintained a constant value ($\kappa \approx 0.4$) for the range of $0 < \beta < 4.66$ but A is changed from 4.7 to 3.3 where it showed deviation from the log-law.

References

[1] Bernard, A., Foucaut, J., Dupont, P. and Stanislas, M., Decelerating boundary layer: a new scaling and mixing length model. *AIAA*, **41 (2)**, 2003, 248-255.

[2] Bourassa, C., Thomas, F.O., An experimental investigation of a highly accelerated turbulent boundary layer, *JFM*, **634**, 2009, 359–404.

[3] Chauhan, K.A., Nagib, H.M. and Monkewitz, P.A., Evidence on non-universality of Kàrmàn constant. In: Proceedings of iTi conference in Turbulence 2005, Springer, Proceedings in Physics, Progress in turbulence II, Part IV, 2007, 159-163.

[4] Chauhan, K.A., Ng, C.H.H. and Marusic, I., Empirical mode decomposition and Hilbert transformations for analysis od oil film interferograms, *Meas. Sci. Technol.*, **21**, 2010.

[5] Clauser, F.H., Turbulent boundary layers in adverse pressure gradients, *J. Aero. Sci.*, **21**, 1954, 91–108.

[6] Dixit, S.A. and Ramesh O.N., Determination of skin friction in strong pressure-gradient equilibrium and near-equilibrium turbulent boundary layers, *Exp. Fluids*, **47**, 2009, 1045–1058.

[7] Fernholz, H.H., Janke, G., Schober, M. and Wagner, P.M., New developments and applications of skin-friction measuring techniques, *Meas. Sci. Technol.*, **7**, 1996, 1396-1409.

[8] Fernholz, H.H. and Warnack, D., The effects of a favourable pressure gradient and of the Reynolds number on an incompressible axisymmetric turbulent boundary layer, *J. Fluid Mech.*, **359**, 1998, 329-356.

[9] Huang, N.E., Zheng, S., Long, S.R., Wu, M.C., Shih, H.H., Zheng, Q., Yen, N., Tung, C.C. and Liu, H.H., The empirical mode decompositin and the Hilbert spectrum for non-linear and non-stationary time series analysis, *Proc. of Royal Soc. A.*, **454**, 1998, 903-995.

[10] Nagano, Y., Tagawa, M. and Tsuji, T., Effects of adverse pressure gradients on mean flows and turbulence statistics in a boundary layer. Proc. 8th Symp. on Turb. Shear Flows, 1991, 7-20.

[11] Nagib, H.M., and Chauhan, K.A., Variations of von Krmn coefficient in canonical flows, *Phisycs of Fluids*, **20**, 2008.

[12] Nickels, T.B., Inner scaling for wall-bounded flows subject to large pressure gradients, *J. Fluid Mech.*, **521**, 2004, 217–239.

[13] Nishizawa, N., Marusic, I., Perry, A.E. and Hornung, H.G., Measurement of wall shear stress in turbulent boundary layers using an optical interferometry method. In: 13th Australian fluid mechanics conference, Monash University, Melbourne, Australia, 1998.

[14] Rüedi, J.D., Nagib, H., Österlund, J. and Monkewitz, P.A., Evaluation of three techniques for wall-shear measurements in three dimensional flows, *Experiments in Fluids*, **35**, 2003, 389–396.

[15] Seto, J. and Hornung, H.G., Two-directional skin friction measurement utilizing a compact internally-mounted thin-liquid-film skin friction meter, *AIAA*, 1993, 93-0180.

[16] Spalart, P.R. and Leonard, A., Direct numerical simulation of equilibrium turbulent boundary layers. In: Durst J *et al*. (eds) Turbulent shear flows, *Springer*, **5**, 1986.

[17] Spalart, P.R. and Watmuff, J.H., Experimental and numerical study of a turbulent boundary layers with pressure gradients, *J. Fluid Mech.*, **249**, 1993, 337-371.

[18] Skåre, P.E. and Krogstad, P.Å, A turbulent equilibrium boundary layer near separation., *J. Fluid Mech.*, **272**, 1994, 319-348.

[19] Tanner, L.H. and Blows, L.G., A study of the motion of oil films on surfaces in air flow, with application to the measurement of skin friction., *J. Phys. E.*, **9**, 1976, 194-202.